Propeptide-Mediated Inhibition of Myostatin Increases Muscle Mass Through Inhibiting Proteolytic Pathways in Aged Mice

Henry Collins-Hooper,[1] Roberta Sartori,[2] Raymond Macharia,[3] Korntip Visanuvimol,[1] Keith Foster,[1] Antonios Matsakas,[4] Hannah Flasskamp,[1] Steve Ray,[5] Philip R. Dash,[1] Marco Sandri,[2] and Ketan Patel[1]

[1]Molecular and Cellular Medicine, School of Biological Sciences, University of Reading, Whiteknights Campus.
[2]Venetian Institute of Molecular Medicine, University of Padova, Italy.
[3]Veterinary Basic Sciences, Royal Veterinary College, London.
[4]Health and Exercise Science, University of Hull.
[5]Natural Biosciences, Whiteknights Campus, Reading.

Address correspondence to Ketan Patel, PhD, School of Biological Sciences, University of Reading, Hopkins Building, Whiteknights Campus, Reading, Berkshire RG6 6UB, UK. Email: ketan.patel@reading.ac.uk

Mammalian aging is accompanied by a progressive loss of skeletal muscle, a process called sarcopenia. Myostatin, a secreted member of the transforming growth factor-β family of signaling molecules, has been shown to be a potent inhibitor of muscle growth. Here, we examined whether muscle growth could be promoted in aged animals by antagonizing the activity of myostatin through the neutralizing activity of the myostatin propeptide. We show that a single injection of an AAV8 virus expressing the myostatin propeptide induced an increase in whole body weights and all muscles examined within 7 weeks of treatment. Our cellular studies demonstrate that muscle enlargement was due to selective fiber type hypertrophy, which was accompanied by a shift toward a glycolytic phenotype. Our molecular investigations elucidate the mechanism underpinning muscle hypertrophy by showing a decrease in the expression of key genes that control ubiquitin-mediated protein breakdown. Most importantly, we show that the hypertrophic muscle that develops as a consequence of myostatin propeptide in aged mice has normal contractile properties. We suggest that attenuating myostatin signaling could be a very attractive strategy to halt and possibly reverse age-related muscle loss.

Key Words: Muscle—Myostatin—Aging—Mouse—Sarcopenia.

Received July 18, 2013; Accepted September 16, 2013

Decision Editor: Rafael de Cabo, PhD

SKELETAL muscle is a highly compliant tissue that undergoes both quantitative and qualitative changes as part of an adaptive process to environmental and physiological stimuli. Skeletal muscle not only serves to produce movement both for locomotion and for the maintenance of posture but also plays a significant role in the metabolic functioning of the body. It also serves as a reservoir of proteins and, working in concert with the liver, acts to control the concentrations of both glucose and amino acids in the circulation (1). A diminution of either the locomotory or metabolic roles in humans leads to a severe attenuation in the quality of life and the predisposition to a number of diseases including diabetes.

The increase in the longevity of individuals in Western societies will present considerable challenges to the health care and economic systems of developed countries as they care for people whose body functions undergo age-related deterioration. Old age is associated with a progressive loss of skeletal muscle mass, a process called sarcopenia (2). Sarcopenia leads to lack of muscle strength and increased fatigability (3), resulting in reduced posture and mobility,

increased risk of falls. These factors all contribute to a decrease in quality of life. At the cellular level, sarcopenic skeletal muscle undergoes progressive muscle fiber atrophy (4) with some evidence for the loss of fast glycolytic fibers (5) and increase in fat and connective tissue (6). At the subcellular level, aged muscle fibers display an increased level of mitochondrial abnormalities and susceptibility to apoptosis. In humans, sarcopenia first becomes evident at middle age. Large population studies have reported that more than 20% of 60- to 70-year olds have sarcopenia and that the number reaches 50% in those aged 75 and older (7). The number of people likely to be affected by sarcopenia will increase dramatically since Western society populations are aging fast, with statisticians predicting that the proportion of people older than 60 years may rise by 40% in the next 30 years. The present burdens on the health care systems to care for individuals suffering from sarcopenia are already huge, estimated to have been about $18.5 billion in 2000, a sum that will increase greatly as number of people afflicted by sarcopenia rises due to aging populations (8). It is, therefore, not surprising that a considerable

effort is being expended to develop antisarcopenic therapies. A number of different strategies have been proposed to halt and/or reserve the adverse effects of sarcopenia. One tranche of research has focused on augmentative programs that normally promote muscle growth, which have included an axis revolving around insulin-like growth factor-1 signaling or testosterone-mediated action (9).

In contrast, we and others have focused on developing muscle growth programs based on attenuating signaling mechanisms that usually inhibit muscle development. One of the most potent inhibitors of muscle development is myostatin, a member of the transforming growth factor-β superfamily of secreted proteins (10). The role of myostatin has been extensively studied in numerous mammalian species including cattle, mice, sheep, dogs, and, in one case, in man. In all cases, inactivation of myostatin results in muscle enlargement through myofiber hypertrophy or hyperplasia or both, together with a reduction in adipose tissue content (11–13). Myostatin initiates an intracellular signaling cascade by firstly binding the extracellular domain of the activin type II receptor, which leads to the recruitment and activation of the activin receptor–like kinases 4 and 5. At least two intracellular signaling cascades have been described that are activated through phosphorylation mediated by the activin receptor–like kinases. Canonical for transforming growth factor-β signaling is the activation by phosphorylation of Smad2/3, enabling an interaction with Smad4 that facilitates entry into the nucleus to activate gene transcription (14). Myostatin can also initiate signaling without the involvement of the Smad2/3 pathway by inhibiting the phosphorylation of Akt, which, in skeletal muscle, acts as nodal point controlling cell proliferation, protein synthesis, and protein catabolism either through the proteasome or autophagy (15). In agreement with its proposed role as being an inhibitor of muscle development, overexpression of myostatin causes muscle loss (16). Higher concentrations of myostatin have been detected in many pathological conditions in which muscle loss is a central feature including HIV and myocardial infarct (reviewed by Matsakas and Diel (17)).

Insights into the mechanisms that control posttranslational modification of myostatin have revealed avenues that permit its neutralization. A key feature is that it is synthesized as an inactive precursor protein, in which an N-terminal propeptide (MyoPPT) is linked via a peptide bond to the C-terminal biologically active region (18). The C-terminal portion only becomes biologically active upon proteolytic processing. However, the MyoPPT is able to associate with of the C-terminal peptide causing a reversion to the latent state (19). We have used this property of the MyoPPT to induce myogenic growth in the whole animal through single injection of adeno-associated virus (AAV) serotype 8 (AAV8)-mediated delivery system into young mice and demonstrated that muscle grew by 55% within 17 weeks (20). Importantly, our virally mediated overexpression of the MyoPPT resulted in the development of many of the phenotypes displayed by the myostatin null mouse, including fiber hypertrophy. Notably in contrast to the myostatin null mouse, the hypertrophic muscle that formed as a consequence of MyoPPT treatment displayed normal levels of specific tension in muscle (21).

Myostatin concentration has been reported to increase in elderly men and women, especially in those showing muscle wasting (22,23). We hypothesize that these elevated concentrations are responsible for age-related muscle loss, and that the MyoPPT will halt the muscle wasting process through its neutralizing activity.

Here, we show that 20-month-old mice given a single injection of MyoPPT resulted in extensive muscle growth within 7 weeks. We provide evidence that muscle mass increased due to a normalization of key genes that control ubiquitin-mediated protein breakdown to levels found in young adult mice. Most importantly, we show that the hypertrophic muscle that developed following MyoPPT treatment was able to generate normal levels of tetanic tension commensurate with its mass.

METHODS

Ethical Approval

Animal work was performed under license from the UK Home Office in agreement with the Animals (Scientific Procedures) Act 1986 and complied with the policy and regulations of the journal.

Animal Maintenance

Healthy male C57Bl/6 mice were bred and maintained according to the NIH Guide for Care and Use of Laboratory Animals, approved by the University of Reading in the Biological Services Unit of Reading University. Mice of either 4 or 20 months old were used for the study. Mice were housed under standard environmental conditions (20–22°C, 12:12-hour light–dark cycle) and provided food and water ad libitum.

Vector Generation

A fragment coding for the modified version of MyoPPT was ligated to cDNA for the mouse IgG2a moiety (18) and cloned into a pDD-derived AAV plasmid under the control of the CAGGs promoter (24). The IgG2a moiety prolongs the half-life of recombinant protein but does not affect muscle growth. All viruses were titered by Nantes Vector Core, France.

Recombinant AAV Administration

To facilitate the injection process, mice were kept at 40°C for 10 minutes to induce vasodilation prior to injection. Six mice at 20 months of age were injected via the tail vein with

2×10^{11} vector genomes (AAV8ProMyo). Animals injected with empty vector served as the untreated group. Wherever indicated, a second control group of 10 young male mice (4 months old) was also examined. Five AAV8ProMyo treated and six animals were weighed at weekly intervals (except Week 6) for 7 weeks after injection (one AAV8ProMyo-treated animal was not weighed weekly due to administrative oversight). Physiological and histological assessments were performed at 7 weeks following recombinant AAV8 administration.

Detection of Transgene Expression From Blood Plasma Samples

Tail vein bleeds (75 μL) were taken at 1, 4, and 7 weeks post-administration of recombinant AAV8 and used to assess transgene expression through western blotting. Plasma samples were diluted in phosphate-buffered saline (1:150), of which 5 μL was denatured in sodium dodecyl sulfate–polyacrylamide gel electrophoresis sample buffer followed by heating at 100°C for 5 minutes. Proteins were resolved using a 4%–12% SDS–NuPAGE (Invitrogen/Novex, Groningen, The Netherlands), prior to blotting onto a ECL-nitrocellulose membrane (Amersham Pharmacia Biotech, UK). Membranes were incubated with goat anti-mouse IgG2a antibody (1:50 dilution; AbD Serotec, UK) followed by an anti-goat horseradish peroxidase secondary antibody (1:3,000 dilution; Sigma, UK). Blots were developed using the ECL detection system (Amersham Pharmacia Biotech). Endogenous myostatin or MyoPPT are not detected with this method.

Histological Analysis

Mice were killed according to Schedule 1 of the Animals Scientific Procedures Act (United Kingdom) prior to the dissection of muscle of interest, were weighed, and then were frozen in liquid nitrogen–cooled isopentane. Frozen muscles were mounted in Tissue Tech freezing medium (Jung) in dry ice–cooled ethanol. Immunocytochemistry was carried out on 10-μm transverse cryosections by firstly air drying for 30 minutes and then blocking in wash buffer (phosphate-buffered saline containing 5% fetal calf serum [vol/vol], 0.05% Triton X-100). All antibodies were diluted in wash buffer 30 minutes before use. Myosin heavy chain (MHC) type I, IIA, and IIB isoforms were identified by using A4.840 IgM (1:1 dilution), A4.74 IgG (1:4 dilution), and BF-F3 IgM (1:1 dilution) supernatant monoclonal primary antibodies (Developmental Studies Hybridoma Bank). Mouse monoclonal antibody against Collagen I from Abcam was used at concentrations of 1:500 for immunohistology. Primary antibodies were visualized using Alexa Fluor 488 goat anti-mouse IgG (1:200; A11029, Molecular Probes) and Alexa Fluor 633 goat anti-mouse IgM (1:200; A21046, Molecular Probes) secondary antibodies. Muscle fiber oxidative capacity was determined by using an succinate dehydrogenase (SDH) staining protocol as described previously (25).

Quantitative PCR

Promega SV Total RNA Isolation kit was used to prepare total RNA from the tibialis anterior muscle (TA) which served as the template for cDNA synthesis generated with Invitrogen SuperScript III Reverse Transcriptase. Quantitative real-time reverse transcription–PCR was performed using Qiagen QuantiTect SYBR Green PCR Kit. All data were normalized to *GAPDH* expression. Primers were designed using the software Primer Express 3.0 (Applied Biosystems) and are listed in Supplementary Table 5.

Muscle Tension Measurements

Dissection of the hind limb was carried out under oxygenated Krebs solution (95% O_2 and 5% CO_2). A silk suture was tied to the distal tendon of the extensor digitorum longus (EDL) with the proximal tendon being left attached to the tibial bone. The leg was pinned to a Sylgard-coated experimental chamber flooded with circulating oxygenated Krebs solution. The silk suture tied to the distal EDL tendon was attached a force transducer (Grass Telefactor FT03). Two silver electrodes were positioned longitudinally on either side of the EDL. The muscle was directly stimulated using an isolated constant voltage stimulator (S48, Grass Telefactor). The EDL was stretched to attain the optimal muscle length, which produced maximum twitch tension (P_t). Tetanic contractions were provoked by stimulus trains of 500-millisecond duration at 10, 20, 50, 100, and 200 Hz. The maximum tetanic tension (P_0) was determined from the plateau of the frequency–tension relationship.

Cross-sectional Area Measurements

Immunofluorescently stained muscle sections were photographed under a 10× lens on a Zeiss Axioimager A1 microscope using a Zeiss Axiocam Mrm camera. Three different photographs were then taken at random on three different sections per muscle per animal. The interactive measurements tool in the Axiovision Rel 4.8 software was then used to process the images to measure their cross-sectional area (CSA). All muscle fibers per fiber type were measured per field of view of the photographs taken (~200 in total).

Statistical Analysis

Data are presented as mean ± *SD*. Significant differences on body weight between groups were determined using multivariate analysis of variance followed by Bonferroni's post hoc test with repeated measurements with time. Wherever applicable, comparisons between two groups were performed by Student's *t* test for independent variables. Differences among groups (old control, old PPT treated, and young control) were analyzed by one-way analysis of variance followed by Bonferroni's multiple comparison tests. Differences were considered statistically significant at $p < .05$.

RESULTS

Single Systemic Injection of AAV8 Virus Expressing Modified Propeptide (AAV8MyoPPT) Results in an Increase in Body and Muscle Mass of Aged Mice

Male C57bl/6 mice (aged 20 months; *n* = 6) were injected with 2×10^{11} vector genomes expressing a stabilized form of the MyoPPT (AAV8MyoPPT). Western blot analysis was used to determine the onset of MyoPPT expression. A strong band of the correct molecular weight was detected in the plasma of animals at all time-points examined commencing from 1 week after injection (data not shown).

The mean body weights were measured for five out of six treated mice and all control mice (*n* = 6) during the 7 weeks of the experiment (save Week 6). During the course of the study, the control-treated animals showed no significant increase in body mass (Figure 1A and B). In contrast, the AAV8MyoPPT-treated mice were 22% heavier than their starting weights at the end of the study (Figure 1A and B). Significant mass increase between the treated and control animals were statistically detectable from Week 5 onwards (Figure 1B; Supplementary Table 1).

We next examined the weights of tissues in the two cohorts to explain body mass differences. There were no significant differences in the weights of either the fat pads or the heart between the two groups when normalized to body mass. However, there were increases in the weights of all four muscle groups investigated (soleus, TA, gastrocnemius, Figure 1C–F and Supplementary Table 2, *n* = 6 for the treated group but not in the controls). We found an apparent muscle-specific response to AAV8MyoPPT with the EDL showing the largest gain in mass (21.42%) and the TA with the smallest increase (6.48%).

Muscle Enlargement Following AAV8MyoPPT Administration Is Caused by Fiber Hypertrophy

Next, we determined the reason underpinning the increase in muscle mass caused by AAV8ProMyo. To that end, we profiled fiber number, myosin heavy chain–specific fiber type size, and fiber type frequency. We found no evidence for changes in fiber number due to the treatment in soleus, EDL, or TA (data not shown). Having found no evidence for an increase in fiber number, we next examined the CSA of fibers in a representative muscle of fast and slow phenotype (EDL and soleus, respectively). There were no type I fibers in the EDL of either the control or treated group. Furthermore, there were no significant differences in the CSA of either type IIA or IIX fibers between AAV8MyoPPT-treated and control mice (Figure 2A and B; Supplementary Table 2a). However, we were able to detect a significant increase of 9.52% in the CSA of type IIB fibers of the EDL following AAV8MyoPPT injection (Figure 2C; Supplementary Table 2a). This change was muscle specific as we found that the soleus had undergone a different set of changes in response to AAV8MyoPPT. Here, the treatment caused a significant decrease in type I fibers CSA (Figure 2D; Supplementary Table 2b) but an increase in the CSA of both the (significant) type IIA (Figure 2E) and (nonsignificant) IIX fibers (Figure 2F). It is also noteworthy that we found an average of 7.3 fibers that were clearly type IIB in the treated group, a feature that was absent in the soleus of the control cohort.

We next investigated the effect of AAV8MyoPPT on fiber type distribution at both the metabolic level and in terms of myosin heavy chain isoform expression. We found a significant decrease of 11.41% in the number of oxidative fibers judged by the expression of SDH in the treated EDL muscle (Figure 2G–I; Supplementary Table 2d). However, we found no evidence of changes in myosin heavy chain expression profile in either the EDL (Figure 2J; Supplementary Table 2c) or soleus apart from the appearance of the few type IIB in the latter muscle as mentioned previously. We next investigated if there was any difference in the connective tissue following treatment with the myostatin propeptide. Immunofluorescent staining of EDL sections for type I collagen revealed there to be no obvious difference between the old control and the old PPT-treated mice (Figure 2K and L). These results show that the increase in muscle mass following to AAV8MyoPPT treatment is not caused by an increase in fiber number but instead due to an enlargement of the fast fibers. Furthermore, a qualitative change was additionally unveiled at least in the EDL muscle following AAV8MyoPPT treatment with a decrease in the proportion of fibers expressing SDH. However, this change in the metabolic status of the muscle was not reflected with changes in the expression of myosin heavy chain. Additionally, unlike in the genetic mutant, there was no change in the endomysial connective tissue compartment following AAV8MyoPPT treatment (26).

Molecular Evidence for Decreased Proteasome-Mediated Polypeptide Breakdown Following AAV8MyoPPT Administration in Aged Mouse

We next examined key markers that would inform on the status of protein breakdown through the proteasome or via autophagy in the TA muscle, which due to its size allows the isolation of a large amount of high-quality RNA needed for our comprehensive molecular profiling.

We examined changes in genes associated with protein breakdown, which may explain muscle enlargement following AAV8MyoPPT administration. We firstly found that the expression of FoxO1, a molecule that promotes the breakdown of protein through both proteasome-mediated polypeptide degradation and autophagy (27,28), was elevated in aged muscle compared with young muscle. However, treatment of old mice with AAV8MyoPPT reduced the concentrations to those found in young muscle (Figure 3A). Subsequently, we examined the response of proteasome
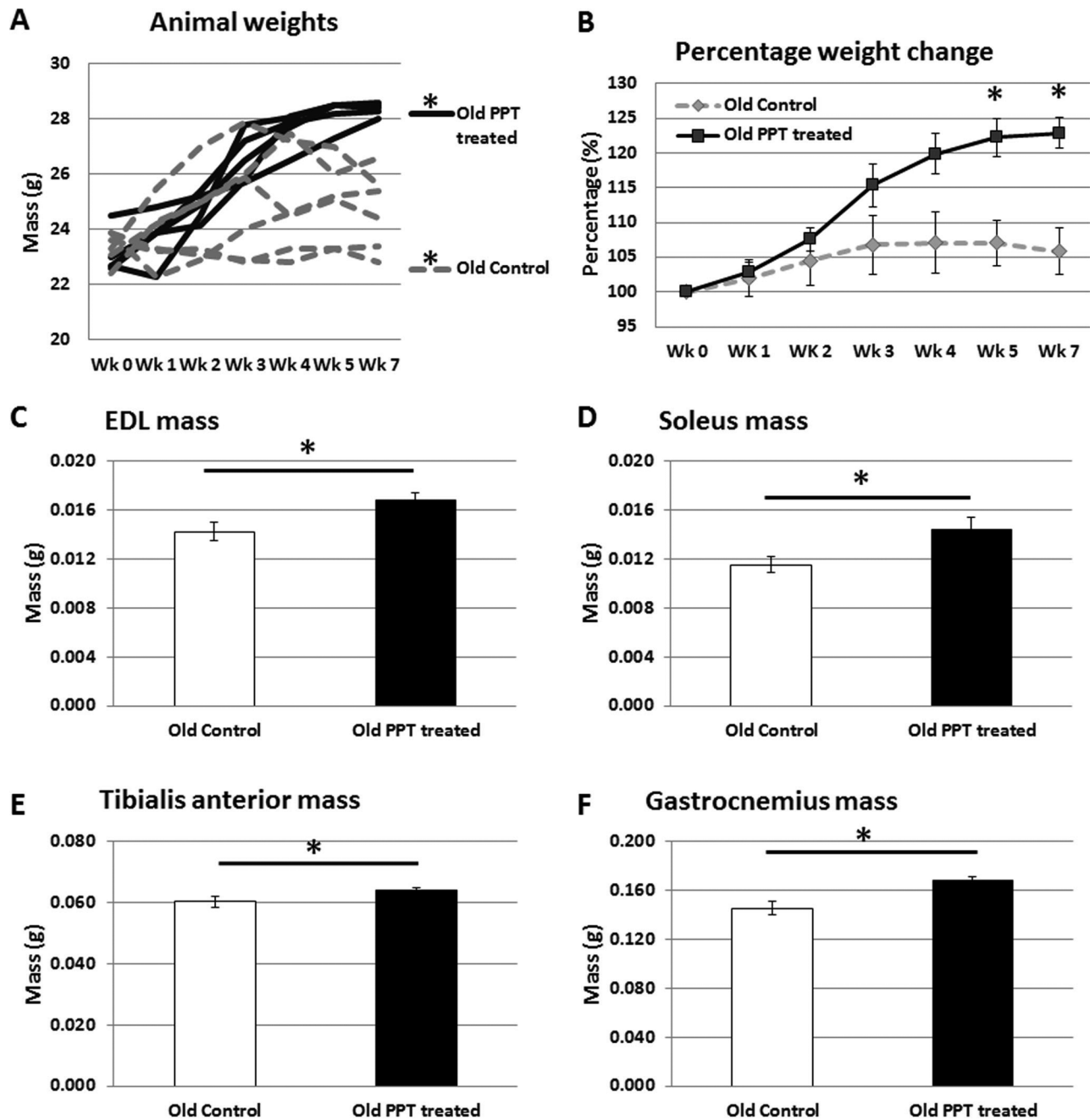
Figure 1. Myostatin propeptide affects whole body and muscle mass in aged mice. (**A**) Myostatin propeptide treatment increases the body mass of aged animals over a 7-week period (multivariate analysis of variance [MANOVA]; *$p < .05$) ($n = 5$ old AAV8ProMyo treated, $n = 6$ old control). (**B**) Myostatin propeptide significantly increased total body mass from 4 weeks after treatment (MANOVA; *$p < .05$) ($n = 5$ old PPT AAV8ProMyo treated, $n = 6$ old control). Myostatin propeptide treatment increased mass of (**C**) EDL, (**D**) soleus, (**E**) tibialis, and (**F**) gastrocnemius after 7 weeks (*$p < .05$). EDL = extensor digitorum longus; PPT = propeptide.

and autophagic pathways to AAV8MyoPPT treatment. We found that the two key ubiquitin ligases, MuRF1 and Atrogin-1, induced by FoxO1 (27) that promote muscle protein breakdown were more abundant in old muscle compared with younger tissue (Figure 3B and C). However, AAV8MyoPPT treatment decreased the expression of both MuRF1 and Atrogin-1 to the concentrations found in young muscle (Figure 3B and C).

Next, we profiled key regulators of autophagy in the TA muscles from old untreated and AAV8MyoPPT-treated samples and compared these to concentrations expressed in young muscle. Here, we studied Bnip3 (inducer of autophagy (29)), Beclin (which promotes the development of the autophagosome, the double membrane vacuole that develops around structures targeted for breakdown (30)), LC3b (protein that controls the development of the
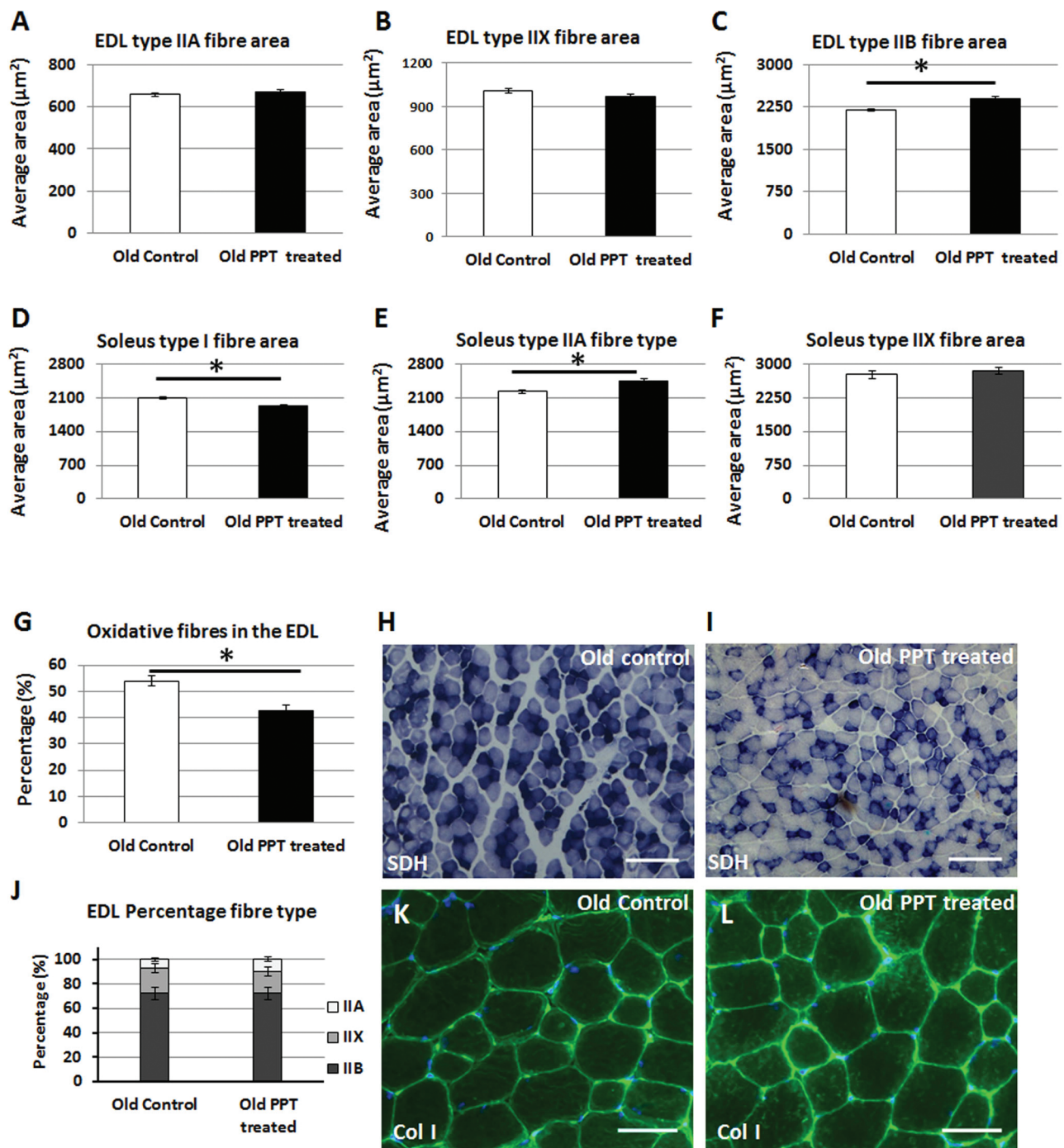
Figure 2. Myostatin propeptide injection in aged mice and muscle fiber characteristics. (**A**) Type IIA and (**B**) type IIX fibers of the EDL did not alter in size to a significant degree following myostatin propeptide treatment. (**C**) Type IIB fibers of the EDL underwent hypertrophy due to myostatin propeptide treatment (*$p < .05$). (**D**) Soleus type I fibers decreased in size following propeptide treatment (*$p < .05$). (**E**) Type IIA fibers of the soleus underwent myostatin propeptide–mediated hypertrophy (*$p < .05$). (**F**) Type IIX fibers of the soleus were unaffected by myostatin propeptide treatment. (**G**) Myostatin propeptide resulted in a decrease in the number of SDH-positive fibers in the EDL. (**H**) SDH activity in old control EDL muscle and (**I**) old AAV8ProMyo-treated EDL muscle. (**J**) Fiber type profiling of EDL muscle from control and AAV8ProMyo-treated animals. No statistically significant changes were detected following treatment. (**K**) Collagen I staining in old control EDL muscle and (**L**) old AAV8ProMyo-treated EDL muscle. Scale bar = 500 µm (H and I). Scale bar = 50 µm (K and L). EDL = extensor digitorum longus; PPT = propeptide; SDH = succinate dehydrogenase.

membrane component of the autophagosome through its ability to undergo lipidation with phosphatidylethanolamine (31)), ATF4 (cysteine protease responsible for cleaving LC3 at its C-terminal arginine residue facilitating the exposed C-terminal glycine to be conjugated to phosphatidylethanolamine (32)), cathepsin L (key lysosomal cysteine endopeptidase required for the degradation of autophagosomal content (33)), Vsp34 (Class III phosphoinositide-3-kinase
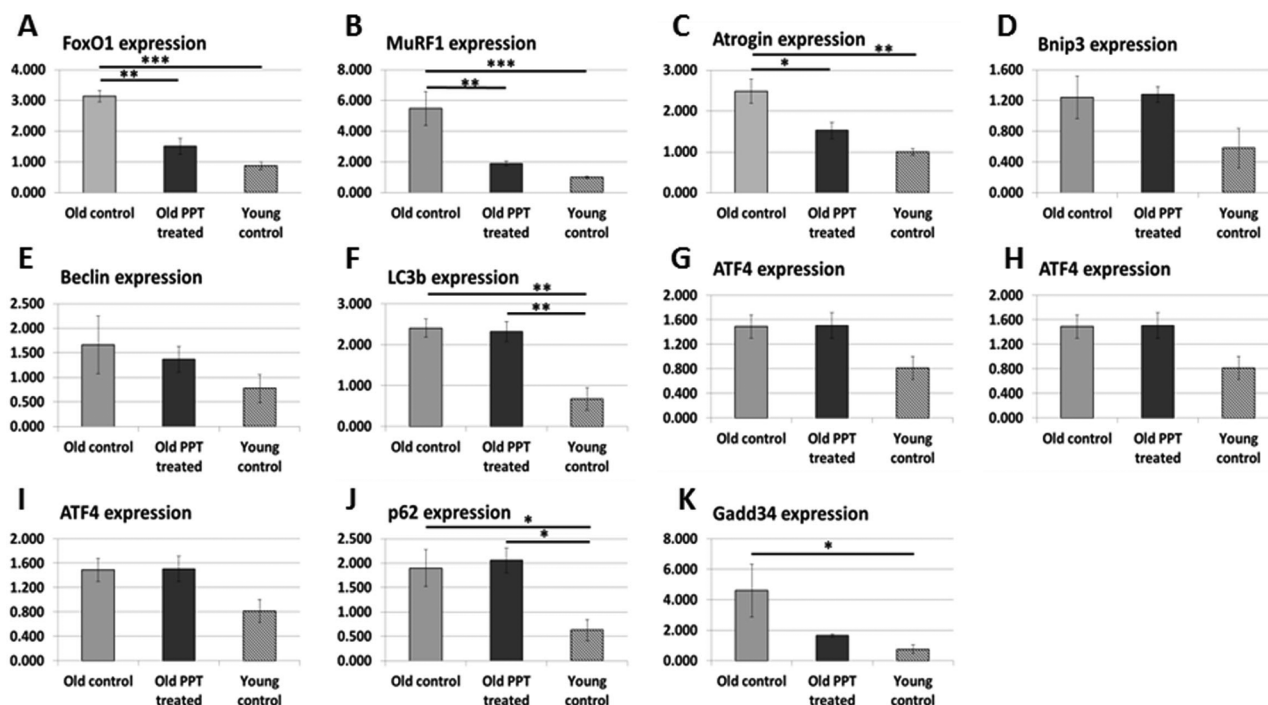
Figure 3. Tibialis anterior gene expression in response to AAV8ProMyo treatment. (**A**) FoxO1. (**B**) MuRF1. (**C**) Atrogin-1. (**D**) Bnip3. (**E**) Beclin. (**F**) LC3b. (**G**) ATF4. (**H**) Cathepsin L. (**I**) Vps34. (**J**) p62. (**K**) Gadd34 (one-way analysis of variance; $*p < .05$, $**p < .001$, $***p < .0001$). PPT = propeptide.

[PI3K] that assembles into multiprotein complexes that include Beclin-1 (34)), and p62 (receptor for cargo destined to be degraded by autophagy (35)). However, there was no general consensus in terms of expression level differences between young and old muscle (Figure 3D, E, and G–I). Secondly, even when a difference did exist, for example, for LC3b and p62 (Figure 3F and J), the concentrations of the autophagic markers were unaltered following AAV8MyoPPT treatment. The only marker of autophagy that did not follow this trend was Gadd34 (which induces autophagy through the suppression of the mTOR pathway (36)) whose expression was normalized to that of young muscle following AAV8MyoPPT treatment (Figure 3K).

Muscle Enlargement Following AAV8MyoPPT Treatment of Aged Mice and Muscle Contraction

Freshly isolated EDL muscles from untreated aged mice and treated mice were physiologically analyzed at 7 weeks post-AAV8MyoPPT injection. Our analysis revealed that maximum twitch tension was increased in treated muscle compared with controls but just failed to reach significant levels (Figure 4A; Supplementary Table 4). However, the maximum tetanic force had increased significantly in older treated muscle (Figure 4C). Furthermore, when both the maximum twitch and maximum tetanic tensions were converted to specific values (taking into account muscle weights), there was no significant difference or even a trend toward a difference in the specific twitch or specific tetanic

tensions between the AAV8MyoPPT-treated and aged control cohorts (Figure 4B and D). These results show that the extra muscle that develops following AAV8MyoPPT treatment is functionally normal.

Conclusions

The prevalence of sarcopenia will increase in the Western world as the control of disease and better nutrition leads to increased life span. Although specific dietary regimes and exercise have been shown to attenuate sarcopenia, at present, we are unable to prevent it from occurring or to restore normal muscle mass following its onset. Many interventions have been proposed to control sarcopenia, but to date, all have only limited success or are accompanied by harmful side effects.

Increasing muscle mass through the control of myostatin-mediated signaling is an attractive strategy since it involves manipulating a naturally occurring mechanism to control muscle mass. This study shows that a single injection of an AAV virus expressing a modified version of the MyoPPT is able to induce muscle growth in aged mice. Importantly, we show through our physiological based experiments that the hypertrophic muscle in aged mice is normal in terms of its ability to generate contraction force. The molecular profiling of key genes indicated that muscle mass has been increased through the normalization of proteasome-mediated polypeptide breakdown to concentrations displayed by young mice that do not display any signs of aging.
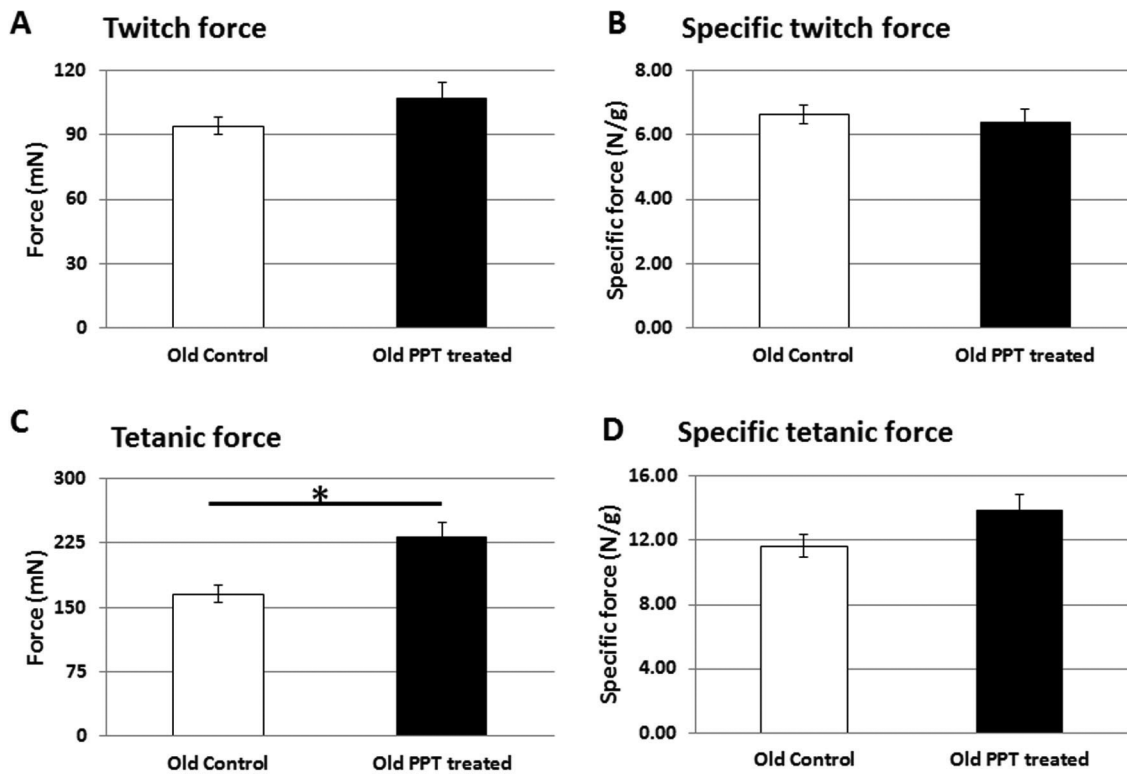
Figure 4. AAV8ProMyo injection in aged mice and EDL muscle contractile properties. (**A**) Maximum twitch force (mN). (**B**) Specific twitch force (maximum twitch tension normalized against muscle wet weight; N/g). (**C**) Maximum tetanic force (mN) (Student's *t* test; *$p < .01$). (**D**) Specific tension (maximum tetanic tension normalized against muscle wet weight, $n = 6$ for each cohort). AAV = adeno-associated virus; EDL = extensor digitorum longus; PPT = propeptide.

This study examined the effect of expressing the myostatin propeptide starting at 20-month-old animals. At this stage, the mice display characteristics of aging including loss in muscle mass (eg, 2 mg decrease in EDL weight between 7 and 20 months of age; see Amthor coworkers (21) and Collins-Hooper, 2013, unpublished data). It is interesting that during the 7 weeks of the study, control-treated mice showed a slight increase in weight, but this was not in the muscle compartment. In contrast, AAV8MyoPPT treatment resulted in increased muscle mass in all entities examined. The small increase in the weight of control-treated animals could be due to fat deposition. However, fat weight changes did not reach significant levels, which could be due to technical difficulties during resection of the entire tissue.

One of the striking findings of this study is that increase in muscle mass brought about by neutralizing myostatin activity resulted in muscle that was capable of generating normal level of tension. This contrasts the situation in the myostatin null, which displays a significant drop in specific tension (21). The differences in terms of specific tension could be explained by considering key features of the karyoplasmatic theory—proposed in 1902 by Robert Hertwig—which postulates that the nuclear to cytoplasmic ratio must be kept with certain values for the optimal functioning of a cell (see Richmond (37) for review of Hertwig's work). The degree of fiber hypertrophy resulting from AAV8MyoPPT treatment does reach the levels caused by genetic deletion of myostatin. We suggest that following AAV8MyoPPT treatment, the nuclear to cytoplasmic ratio does not drop to the detrimental levels found in the knockout mouse model.

We have previously shown that AAV8MyoPPT treatment was able to induce robust growth to some but not all muscles in young mice. That work was conducted on mice of 6 weeks of age treated for 8 weeks and reported an increase in the weights of the TA, gastrocnemius, and EDL of 25%, 27%, and 15% respectively. The soleus did not increase mass in a statistically significant manner (20). However, in a study using essentially the same reagents by an independent laboratory reported that the AAV8MyoPPT was effective in young mice but not in adult mice (38). This leads to the hypothesis that the intervention window for inducing muscle growth by antagonizing the action of myostatin may be limited to relatively early postnatal life. However, this study and that of others suggest that this conclusion is incorrect as the attenuation of myostatin-mediated signaling through at least two approaches leads to increased muscle mass in aged mice. The ultimate basis for the success of these strategies must rely on the age-related increased expression of myostatin. Some studies have shown no change in myostatin with aging, whereas others have actually reported a decrease myostatin transcript (39,40). However, a recent study has shown for the first time an increase in both mRNA and myostatin protein in an aged human cohort (23). Many of the spurious results can be attributed to using nonspecific

reagents especially antibodies purporting to be specific to myostatin.

Our previous study reported an increase in mass of 25%, 27%, and 15% for the TA, gastrocnemius, and EDL, respectively, and a nonsignificant enlargement of 13% for the soleus in 14-week-old mice (20). Here, we report significant mass gains of 7%, 16%, 21%, and 17% for the TA, gastrocnemius, EDL, and soleus, respectively, in 87-week-old mice. Therefore, two muscles have increased mass to a greater extent in old mice (EDL and soleus) and two display smaller increases (TA and gastrocnemius). Although it is beyond doubt that the AAV8MyoPPT treatment has induced increases in mass of all examined muscles in aged animals, the mechanisms that control the relative growth muscles are not easy to pin down using this set of data due to the differences in genetic background of the mice used in the two studies.

Two recent studies have used a protocol of multiple anti-myostatin antibody injections to increase muscle mass in aged mice. The results from those studies and findings reported here are worthy of comparison. The study of LeBrasseur and coworkers deployed a weekly injection regime of a high (25 mg/kg) of the PF-345, an anti-myostatin antibody, on 24-month-old mice for 4 weeks (41). The mice in their study did not increase their body weights but did show muscle growth (gastrocnemius had increased in mass by 12%). Murphy and colleagues (42) used the same antibody at a lower dose (10 mg/kg) for 14 weeks on 18-month-old mice and reported an increase in the mass of soleus, gastrocnemius, and quadriceps of 18%, 8%, and 9%, respectively. However, the EDL and TA did not show a significant enlargement. Interestingly, both antibody regimes induced an increase in an oxidative profile and, in the study of Murphy and colleagues, a fiber type shift toward IIA. In contrast, we have shown that a single injection of the AAV8MyoPPT treatment leads to significantly increased enlargement of all muscles examined (EDL: 21%; gastrocnemius: 16%; soleus: 17%; and TA: 7%). These differences could be attributed to a number of reasons. It is likely that the differing structures of the two molecules is going to impact on the degree of tissue infiltration by the antagonizing molecule influenced through their interaction with the local connective tissue, whose composition differs based on the muscle fiber profile. Alternatively, the MyoPPT could neutralize proteins in addition to myostatin, which share functional and structural homology, for example, activin. Finally, the differences in efficacy could simply be due to the delivery protocol. We have used a viral method that leads to infection of cells and the sustained production of the neutralizing agent, which may attain higher concentrations of the active molecule compared to the injection procedures.

However, one major difference in the outcomes of the antibody-based studies and this investigation is that concerning the effect on the metabolic profile of muscle. We show that AAV8MyoPPT treatment leads to a decrease in the number of SDH-positive fibers, whereas antibody-mediated myostatin leads to an increase in the oxidative profile. Our results are in agreement with the phenotype of the myostatin null mouse, dog, and cattle breeds, which all display increased number of glycolytic fibers (21). Interestingly, we were unable to detect a change in the myosin heavy chain profile toward a fast phenotype, even though there was a change in terms of the metabolic profile. This finding can be explained by taking into account that SDH concentrations can be manipulated quite rapidly (43), for example, over a few days through exercise regimes, whereas MHC turnover rates are in the order of many weeks (44).

The mechanism by which AAV8MyoPPT treatment results in increased muscle growth in aged animals seems to be similar to that regulated by the anti-myostatin antibody. In both cases, there was a decrease in the expression of MuRF1 and Atrogin-1 key muscle E3 ubiquitin ligases (27). However, we also report that aged muscle has an increased expression of FoxO1, which is able to induce not only proteasome-mediated degradation but also autophagy. Here, we show that there is an increase in both major muscle E3 ubiquitin ligases (MuRF1 and Atrogin-1) in aged muscle compared with young muscle. Furthermore, the expression of both these genes is significantly reduced through AAV8MyoPPT treatment, suggesting that suppression of protein breakdown through the proteasome should be targeted to develop antisarcopenic regimes. In contrast, we did not find a strong case for autophagy being clearly activated at a greater level in aged muscle, which is in agreement with numerous other studies. Indeed this has led some to suggest that autophagy plays a tissue-specific role during aging with some organs being more susceptible to damage through this mechanism (eg, liver and heart (45)) than others, possibly including skeletal muscle (46).

Myostatin is firmly established as a negative regulator of muscle growth. However, there is less agreement about how this activity is mediated. One school of thought is that it acts to suppress the activity of skeletal muscle stem cells (47). In contrast, others have conclusively shown that myostatin inhibits muscle enlargement and regeneration by controlling protein synthesis and breakdown in myofibers, through a mechanism largely if not wholly independent of satellite cells (48,49). These differing modes of action will have profound implication in terms of using myostatin antagonists to treat sarcopenia since we and others have shown that the number of stem cells declines drastically with age (50). Therefore, any mechanism promoting muscle growth though the activation of resident satellite cells is likely to be less efficacious with age. However, an elegant genetic-based study has recently shown that ablation of satellite cells does not prevent muscle hypertrophy in the absence of myostatin. Therefore, we suggest that the major means of muscle enlargement has been brought about in this study is through an acellular hypertrophic response. Therefore, myostatin inhibition offers an attractive means to increase muscle mass not only when a depletion of satellite cells

occurs in an aging context but also in a spectrum of muscle diseases in which this population is diminished.

In summary, a striking level of muscle growth is induced by antagonizing myostatin signaling by the overexpression of the myostatin propeptide in aged mice. This work shows that aged muscle can be induced to undergo an increase in mass, and that the resultant tissue is capable of generating normal levels of force. We demonstrate that the muscle grew by increasing the size of existing fibers and was not likely to dependent on resident stem cells. Furthermore, we showed that the muscle had decreased its oxidative profile, which would lend itself to greater glucose use. These manifestations imply that myostatin propeptide halts and reverses the adverse effects of sarcopenia in terms of muscle mass and the metabolic changes associated with aging muscle (37).

Supplementary Material

Supplementary material can be found at: http://biomedgerontology.oxfordjournals.org/

References

1. Spargo E, Pratt OE, Daniel PM. Metabolic functions of skeletal muscles of man, mammals, birds and fishes: a review. *J R Soc Med*. 1979;72:921–925.
2. Cruz-Jentoft AJ, Baeyens JP, Bauer JM, et al.; European Working Group on Sarcopenia in Older People. Sarcopenia: European consensus on definition and diagnosis: report of the European Working Group on Sarcopenia in Older People. *Age Ageing*. 2010;39:412–423.
3. Faulkner JA, Brooks SV, Zerba E. Skeletal muscle weakness and fatigue in old age: underlying mechanisms. *Annu Rev Gerontol Geriatr*. 1990;10:147–166.
4. Faulkner JA, Brooks SV, Zerba E. Muscle atrophy and weakness with aging: contraction-induced injury as an underlying mechanism. *J Gerontol A Biol Sci Med Sci*. 1995;50 Spec No:124–129.
5. Alnaqeeb MA, Goldspink G. Changes in fibre type, number and diameter in developing and ageing skeletal muscle. *J Anat*. 1987;153:31–45.
6. Marshall PA, Williams PE, Goldspink G. Accumulation of collagen and altered fiber-type ratios as indicators of abnormal muscle gene expression in the mdx dystrophic mouse. *Muscle Nerve*. 1989;12:528–537.
7. Berger MJ, Doherty TJ. Sarcopenia: prevalence, mechanisms, and functional consequences. *Interdiscip Top Gerontol*. 2010;37:94–114.
8. Janssen I, Shepard DS, Katzmarzyk PT, Roubenoff R. The healthcare costs of sarcopenia in the United States. *J Am Geriatr Soc*. 2004;52:80–85.
9. Giannoulis MG, Martin FC, Nair KS, Umpleby AM, Sonksen P. Hormone replacement therapy and physical function in healthy older men. Time to talk hormones? *Endocr Rev*. 2012;33:314–377.
10. McPherron AC, Lawler AM, Lee SJ. Regulation of skeletal muscle mass in mice by a new TGF-beta superfamily member. *Nature*. 1997;387:83–90.
11. McPherron AC, Lee SJ. Double muscling in cattle due to mutations in the myostatin gene. *Proc Natl Acad Sci USA*. 1997;94:12457–12461.
12. Schuelke M, Wagner KR, Stolz LE, et al. Myostatin mutation associated with gross muscle hypertrophy in a child. *N Engl J Med*. 2004;350:2682–2688.
13. Clop A, Marcq F, Takeda H, et al. A mutation creating a potential illegitimate microRNA target site in the myostatin gene affects muscularity in sheep. *Nat Genet*. 2006;38:813–818.
14. Tsuchida K. The role of myostatin and bone morphogenetic proteins in muscular disorders. *Expert Opin Biol Ther*. 2006;6:147–154.
15. Trendelenburg AU, Meyer A, Rohner D, Boyle J, Hatakeyama S, Glass DJ. Myostatin reduces Akt/TORC1/p70S6K signaling, inhibiting myoblast differentiation and myotube size. *Am J Physiol Cell Physiol*. 2009;296:C1258–C1270.
16. Zimmers TA, Davies MV, Koniaris LG, et al. Induction of cachexia in mice by systemically administered myostatin. *Science*. 2002;296:1486–1488.
17. Matsakas A, Diel P. The growth factor myostatin, a key regulator in skeletal muscle growth and homeostasis. *Int J Sports Med*. 2005;26:83–89.
18. Wolfman NM, McPherron AC, Pappano WN, et al. Activation of latent myostatin by the BMP-1/tolloid family of metalloproteinases. *Proc Natl Acad Sci USA*. 2003;100:15842–15846.
19. Hill JJ, Davies MV, Pearson AA, et al. The myostatin propeptide and the follistatin-related gene are inhibitory binding proteins of myostatin in normal serum. *J Biol Chem*. 2002;277:40735–40741.
20. Matsakas A, Foster K, Otto A, et al. Molecular, cellular and physiological investigation of myostatin propeptide-mediated muscle growth in adult mice. *Neuromuscul Disord*. 2009;19:489–499.
21. Amthor H, Macharia R, Navarrete R, et al. Lack of myostatin results in excessive muscle growth but impaired force generation. *Proc Natl Acad Sci USA*. 2007;104:1835–1840.
22. Gonzalez-Cadavid NF, Taylor WE, Yarasheski K, et al. Organization of the human myostatin gene and expression in healthy men and HIV-infected men with muscle wasting. *Proc Natl Acad Sci USA*. 1998;95:14938–14943.
23. McKay BR, Ogborn DI, Bellamy LM, Tarnopolsky MA, Parise G. Myostatin is associated with age-related human muscle stem cell dysfunction. *FASEB J*. 2012;26:2509–2521.
24. Yue Y, Dongsheng D. Development of multiple cloning site cis-vectors for recombinant adeno-associated virus production. *BioTechniques*. 2002;33:672, 674, 676–672, 674, 678.
25. Matsakas A, Macharia R, Otto A, et al. Exercise training attenuates the hypermuscular phenotype and restores skeletal muscle function in the myostatin null mouse. *Exp Physiol*. 2012;97:125–140.
26. Elashry MI, Collins-Hooper H, Vaiyapuri S, Patel K. Characterisation of connective tissue from the hypertrophic skeletal muscle of myostatin null mice. *J Anat*. 2012;220:603–611.
27. Sandri M, Sandri C, Gilbert A, et al. Foxo transcription factors induce the atrophy-related ubiquitin ligase atrogin-1 and cause skeletal muscle atrophy. *Cell*. 2004;117:399–412.
28. Sandri M. FOXOphagy path to inducing stress resistance and cell survival. *Nat Cell Biol*. 2012;14:786–788.
29. Tracy K, Macleod KF. Regulation of mitochondrial integrity, autophagy and cell survival by BNIP3. *Autophagy*. 2007;3:616–619.
30. Liang XH, Jackson S, Seaman M, et al. Induction of autophagy and inhibition of tumorigenesis by beclin 1. *Nature*. 1999;402:672–676.
31. Tanida I, Ueno T, Kominami E. LC3 and Autophagy. *Methods Mol Biol*. 2008;445:77–88.
32. Kirisako T, Ichimura Y, Okada H, et al. The reversible modification regulates the membrane-binding state of Apg8/Aut7 essential for autophagy and the cytoplasm to vacuole targeting pathway. *J Cell Biol*. 2000;151:263–276.
33. Dennemärker J, Lohmüller T, Müller S, et al. Impaired turnover of autophagolysosomes in cathepsin L deficiency. *Biol Chem*. 2010;391:913–922.

34. Furuya T, Kim M, Lipinski M, et al. Negative regulation of Vps34 by Cdk mediated phosphorylation. *Mol Cell*. 2010;38:500–511.

35. Pursiheimo JP, Rantanen K, Heikkinen PT, Johansen T, Jaakkola PM. Hypoxia-activated autophagy accelerates degradation of SQSTM1/p62. *Oncogene*. 2009;28:334–344.

36. Uddin MN, Ito S, Nishio N, Suganya T, Isobe K. Gadd34 induces autophagy through the suppression of the mTOR pathway during starvation. *Biochem Biophys Res Commun*. 2011;407:692–698.

37. Richmond ML. Protozoa as precursors of Metazoa: German cell theory and its critics at the turn of the century. *J Hist Biol*. 1989;22:243–276.

38. Qiao C, Li J, Jiang J, et al. Myostatin propeptide gene delivery by adeno-associated virus serotype 8 vectors enhances muscle growth and ameliorates dystrophic phenotypes in mdx mice. *Hum Gene Ther*. 2008;19:241–254.

39. Carlson ME, Hsu M, Conboy IM. Imbalance between pSmad3 and Notch induces CDK inhibitors in old muscle stem cells. *Nature*. 2008;454:528–532.

40. Haddad F, Adams GR. Aging-sensitive cellular and molecular mechanisms associated with skeletal muscle hypertrophy. *J Appl Physiol*. 2006;100:1188–1203.

41. LeBrasseur NK, Schelhorn TM, Bernardo BL, Cosgrove PG, Loria PM, Brown TA. Myostatin inhibition enhances the effects of exercise on performance and metabolic outcomes in aged mice. *J Gerontol A Biol Sci Med Sci*. 2009;64:940–948.

42. Murphy KT, Koopman R, Naim T, et al. Antibody-directed myostatin inhibition in 21-mo-old mice reveals novel roles for myostatin signaling in skeletal muscle structure and function. *FASEB J*. 2010;24:4433–4442.

43. McPhail LC, Cunningham CC. The role of protein and lipids in stabilizing the activity of bovine heart succinate dehydrogenase. *Biochemistry*. 1975;14:1122–1131.

44. Papageorgopoulos C, Caldwell K, Schweingrubber H, Neese RA, Shackleton CH, Hellerstein M. Measuring synthesis rates of muscle creatine kinase and myosin with stable isotopes and mass spectrometry. *Anal Biochem*. 2002;309:1–10.

45. Wohlgemuth SE, Julian D, Akin DE, et al. Autophagy in the heart and liver during normal aging and calorie restriction. *Rejuvenation Res*. 2007;10:281–292.

46. Wohlgemuth SE, Seo AY, Marzetti E, Lees HA, Leeuwenburgh C. Skeletal muscle autophagy and apoptosis during aging: effects of calorie restriction and life-long exercise. *Exp Gerontol*. 2010;45:138–148.

47. Thomas M, Langley B, Berry C, et al. Myostatin, a negative regulator of muscle growth, functions by inhibiting myoblast proliferation. *J Biol Chem*. 2000;275:40235–40243.

48. Lee SJ, Huynh TV, Lee YS, et al. Role of satellite cells versus myofibers in muscle hypertrophy induced by inhibition of the myostatin/activin signaling pathway. *Proc Natl Acad Sci USA*. 2012;109:E2353–E2360.

49. Amthor H, Otto A, Vulin A, et al. Muscle hypertrophy driven by myostatin blockade does not require stem/precursor-cell activity. *Proc Natl Acad Sci USA*. 2009;106:7479–7484.

50. Collins-Hooper H, Woolley TE, Dyson L, et al. Age-related changes in speed and mechanism of adult skeletal muscle stem cell migration. *Stem Cells*. 2012;30:1182–1195.